Form constraints in motion binding

Jean Lorenceau[1,2] and David Alais[1,2]

[1] Unité de Neurosciences Intégratives et Computationnelles, UPR 2191 CNRS, Avenue de la Terrasse, Gif-sur-Yvette 91198, France

[2] Laboratoire de Physiologie de la Perception et de l'Action, Collège de France, 75005 Paris, France

Correspondence should be addressed to J.L. (lorenceau@iaf.cnrs-gif.fr)

Visual analyses of form and motion proceed along parallel streams. Unified perception of moving forms requires interactions between these streams, although whether the interactions occur early or late in cortical processing remains unresolved. Using rotating outlined shapes sampled through apertures, we showed that binding local motions into global object motion depends strongly on spatial configuration. Identical local motion components are perceived coherently when they define closed configurations, but usually not when they define open configurations. Our experiments show this influence arises in early cortical levels and operates as a form-based veto of motion integration in the absence of closure.

A popular view of cortical processing suggests that visual stimuli pass through parallel ventral and dorsal streams specialized for form and motion, often respectively referred to as 'what' and 'where' pathways[1–4] (but see ref. 5). From primary visual cortex, the 'what' stream ascends ventrally to inferotemporal cortex, and the 'where' stream continues dorsally to posterior parietal cortex. This functional dichotomy raises the question of how a unified perception of moving objects emerges and whether it results from interactions between these streams.

Psychophysical studies addressing this question provide evidence for the existence of form–motion interactions, with data suggesting they are reciprocal in nature[6,7] and that they occur at relatively high levels[8]. Whereas this conclusion squares with neurophysiological evidence for a late integration of form and motion in prefrontal cortex[9], there is also data suggesting early interactions in primary visual cortex[10–12]. Here we challenge the view that form–motion interactions occur between late 'what' and 'where' areas, and we provide psychophysical evidence that form has a profound and early influence on the binding of local motions into global motion.

In previous experiments, we studied motion binding using an outline diamond globally rotating behind an occluding surface. The occluder contained small apertures that revealed the diamond's contours but left the vertices hidden (**Fig. 1c**). Despite each of the contours being directionally ambiguous and lacking a rotational component, observers could easily perceive the diamond's rotation[13–17]. The ability to recover the coherent global motion is usually considered in terms of spatiotemporal integration of local motions. However, an influence of form perception not addressed by this account is that when subjects perceive coherent global motion, they also experience a coherent global form—an occluded diamond-shaped surface undergoing rotation. Conversely, if they do not perceive a global form behind the occluding surface, they perform poorly at discriminating the direction of global rotation.

The concomitant perception of form and motion in the occluded diamond provided our starting point and motivated us to try to disentangle these covarying stimulus attributes. To this end, the present experiments again use the aperture-viewing protocol, but the stimulus set has been expanded (**Fig. 1a**) to include other shapes (such as diamonds, bow-ties and crosses). As before, the shapes were rigid, and all vertices were hidden by the occluder, so that the rotating shapes were reduced to a sample of four oscillating contours with no rotational component. The shapes were chosen so that they would yield identical local motion components when viewed through the apertures, and all had very similar spatial energy spectra (**Fig. 1b** and **d**). With the spatiotemporal content of the stimuli matched, they are distinguished simply by the spatial layout of their contours and the form of the occluded shape they imply.

Theories of global motion based on intersecting constraint lines[18] or vector sums[19] predict that spatiotemporal integration of the ambiguous local motions would suffice to recover object motion, regardless of geometrical structure. Yet the spatial arrangement of the contours may be important, as some shapes (such as the diamonds) can be resolved into closed, bounded objects through processes such as amodal contour completion. This is not true of other shapes (such as the cross, arrow and chevron) whose contours project in parallel or radiate without intersecting. Our data did indeed show a strong dependence on shape; performance was much better for the diamond-like shapes. Moreover, for shapes yielding poor performance, neither extensive practice nor previous knowledge of the full, unoccluded shape improved performance. Together, this suggests that form strongly influences global motion perception, and does so at a low level.

Results

In experiment 1, observers' performance on the global motion task—discriminating clockwise versus counterclockwise circular translation for ten shapes (see Methods)—was measured over eight sessions. Despite all stimuli being very similar (or identical) in their two-dimensional spatial frequency space and velocity space representations (**Fig. 1b** and **d**), performance varied widely. When ranked by performance (**Fig. 2a**), two homogenous shape categories emerged: those yielding good performance (greater than 90%) and those yielding poor performance (less than 75%). Confirming this dichotomy, all pair-wise comparisons (Tukey's HSD) between but not within the 'easy' (>75% correct) and 'difficult' (<75% correct) groups were significant. Plotting these data by session (**Fig. 2b**, left) reveals that

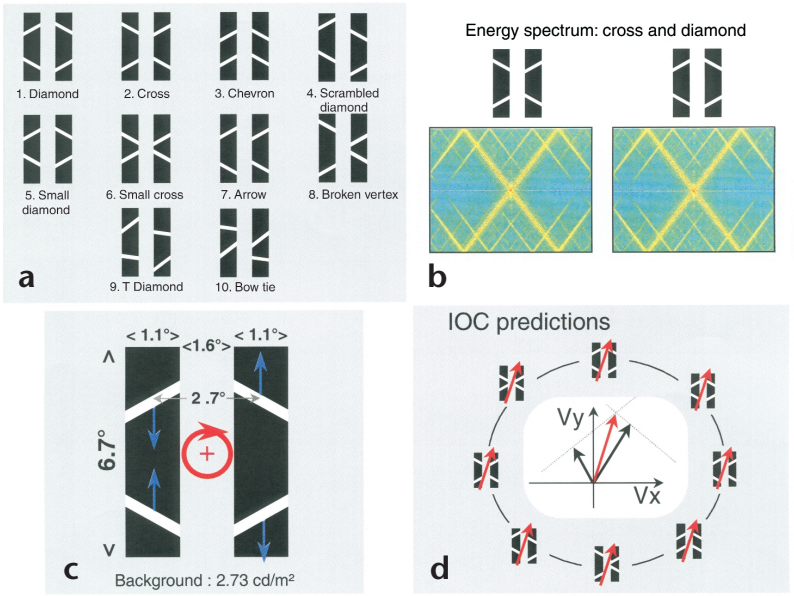

Fig. 1. Stimuli used in the experiments. (**a**) Occluded versions of the shapes used in the experiments. The occluded stimuli underwent a rigid global circular translation. Observers judged whether rotation was clockwise or counter-clockwise. All shapes were derived from a single diamond stimulus by permuting one or more component contours (1, 2, 3, 5, 6, 7), by adding a vertical offset (4, 8) or by rotating the contours (9, 10). Permutations maintain the distance between segments, but change the overall segment configuration. Vertical offsets maintain the global form but change the distances between segments. Rotations maintain the distance between segments, but alter both the relatability between segments and the orientational content of the stimuli. We evaluate the influence of these shape modifications on spatiotemporal integration for matched motion components (shapes 1–8 had identical local motions). (**b**) Because shape modifications change only the contour locations, the energy spectra of all stimuli are essentially identical; only the phase spectra (data not shown) are different. (**c**) Translating the stimuli around a circular path produces up-and-down oscillations of the visible segments with no rotational component. Spatiotemporal integration of contour motions is necessary to discriminate rotation direction. (**d**) Predictions of global motion direction derived from an intersection of constraints (IOC) rule[18] are identical for all shapes at any moment during rotation. (For clarity, predictions for stimuli 9 and 10 are not shown.) Using a vector-sum rule would also produce identical predictions for all shapes.

this shape-based dichotomy extends to perceptual learning. For the four 'easy' shapes, for which performance was already good in the first session, performance improved with practice ($F_{7,14} = 3.69$, $p < 0.018$), whereas practice did not improve performance for the six 'difficult' shapes ($F_{7,14} = 2.1$, n.s.). Continued practice for a further five sessions with feedback (**Fig. 2b**, right) also failed to improve performance ($F_{1,2} = 2.38$, n.s.). We then measured perceived coherence for the diamond, cross and chevron shapes. In a long series of paired comparisons[20], observers judged which shape was more coherent. The obtained proportions, converted to standard units (mean, 0; s.d., 1) on a 'perceived coherence' dimension are as follows: diamond, 0.87 ± 0.09; cross, –0.06 ± 0.04; chevron, –0.81 ± 0.07. This matches the order for the rotation data, pointing to a strong relationship between perceived coherence and performance on the global rotation task.

In velocity space, all shapes in Fig. 1 are composed of just two motion vectors (**Fig. 1d**). To test whether increasing the number of motion components available for spatiotemporal integration would facilitate global motion discrimination for 'difficult' shapes, we created five new shape variants containing three or four motion components (**Fig. 3a**), all of which are consistent with a single global motion solution. Significantly, these shapes also vary in the degree of closure implied in the occluded form, with shapes one and two implying closed, convex forms, and shapes four and five implying open, concave forms. The data clearly show that providing the motion system with more information does not boost performance for difficult shapes. Stimuli one and five (and two and four) have identical motion components, and yet performance is at ceiling for the former and at chance for the latter. Again, the closed, convex forms yield good performance.

It is possible that the apparent form-based distinction results from a lack of familiarity with concave, open shapes, making it hard to visualize the occluded form. If this were so, the difficulty might be overcome by showing the observer the complete shape before each trial. We therefore presented the complete diamond, cross and chevron stimuli (**Fig. 3b**) as static primes in front of the occluders for one second. Immediately after the prime

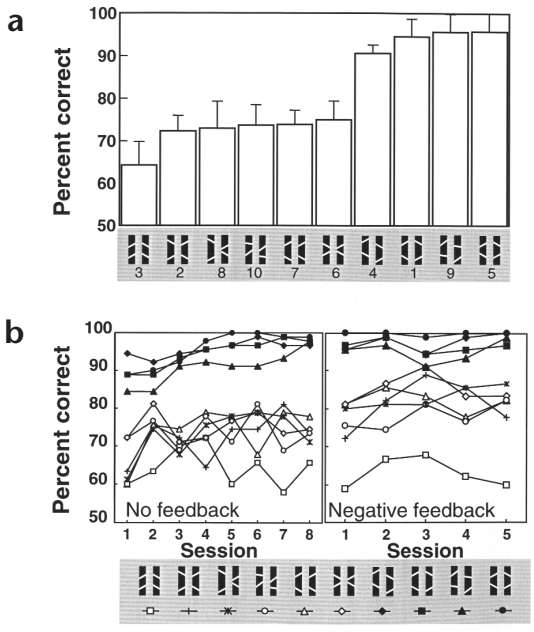

Fig. 2. Motion binding with different shapes. (**a**) Data pooled across two directions, eight experimental sessions and across observers, ranked by performance. Statistical analysis reveals two distinct categories: four 'easy' shapes (performance above 90% correct) and six 'difficult' shapes (performance below 75% correct). The numbers along the abscissa refer to the shapes shown in Fig. 1a. (**b**) Left, data from (**a**) plotted by session. Significant learning is seen for the 'easy' shapes but not for 'difficult' shapes. Right, additional data from five extra sessions with feedback shows no further learning effect. Each data point is the average of 40 trials.

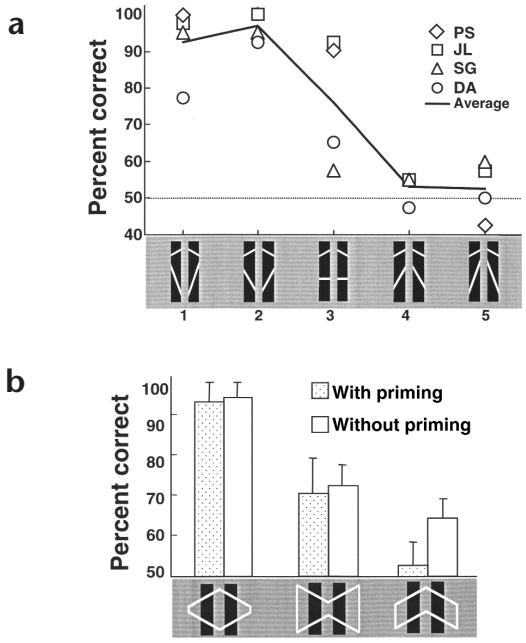

Fig. 3. Motion binding with four-component stimuli. (**a**) Bottom, five shapes used in the experiment. The component vectors for all shapes can be resolved into a single intersection of constraint (IOC) or vector-sum direction. Shapes 1 and 5 (and 2 and 4) were constructed by exchanging the location of the lower segments. This has the effect of varying the nature of the occluded shape. From left to right, the shapes vary from closed and convex to open and concave. This was achieved by rotating the lower contours inward. Thus, shape 3, the triangle, is intermediate between open and closed forms. Top, direction discrimination performance for each of the five shapes. Performance is close to ceiling for closed shapes and near chance level for open shapes. These shapes comprise four (or three) motion components, thus providing a better sample of the global rotation, yet this does not help rotation discrimination for open shapes. (**b**) Effect of priming. Observers were presented the full outline of the static shape for one second, before occluded rotation began. For comparison, performance with priming (light texture) is shown with the results without priming (no texture). Priming the observer with the exact form of the occluded shape does not improve performance for open shapes.

period expired, the shapes were moved behind the occluders and the global rotation began. Although observers became very familiar with the shapes (each was presented a hundred times per block), this did not facilitate global rotation discrimination for difficult shapes (**Fig. 3b**).

The absence of priming and learning effects suggests that shape exerts an early influence on motion binding, rather than a late one. If so, altering low-level stimulus properties might influence performance on the rotation task. Early cortical processing of motion and form is often discussed in terms of magnocellular and parvocellular pathways. These subcortical streams carry information to primary visual cortex and provide inputs to the ventral 'form' and dorsal 'motion' pathways[21–23]. Because of their different specializations, magno and parvo cells respond differentially to contrast, and to temporal and spatial frequency. The following experiments capitalize on these differences to create stimuli that will favor the magnocellular path at the expense of parvocellular path. This was done by reducing contour luminance and doubling rotation speed or by introducing Gaussian-profile contours of various widths to manipulate spatial frequency. Given that performance differences among the shapes seem to be a matter of geometrical form, we expected that conditions unfavorable to form processing would reduce the distinction between 'easy' and 'difficult' shapes.

Results reveal that reducing contour luminance dramatically improves rotation discrimination for difficult shapes, with mean performance reaching 91% correct for the cross and chevron (**Fig. 4a**). Presumably, performance for the diamond would also improve if it were not already at ceiling. To verify this, we repeated the experiment with gray (invisible) apertures (**Fig. 4b**). When apertures are invisible, contour terminators are classified as intrinsic (rather than extrinsic, the result of occlusion), which disambiguates the motion of the contours and renders their integration more difficult[13,24]. This manipulation did indeed reduce performance from ceiling, revealing improving

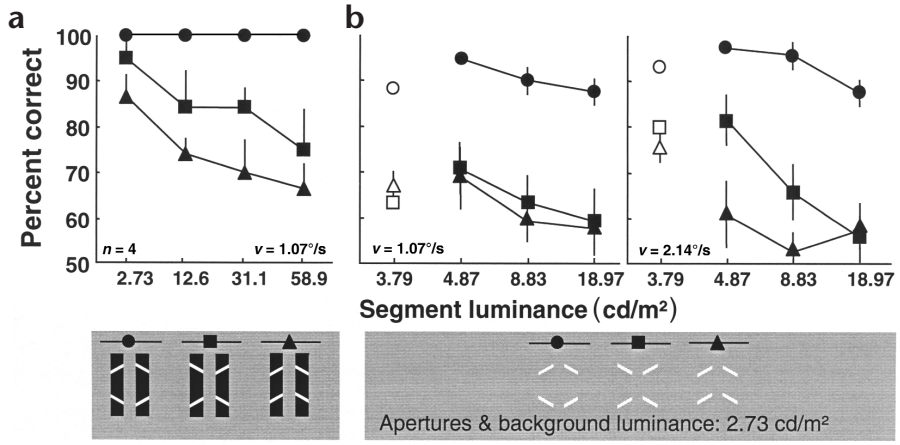

Fig. 4. Rotation discrimination as a function of segment luminance. (**a**) With (visible) black apertures presented within a gray background, performance for the cross and chevron improves as segment luminance decreases. Performance for the diamond is at ceiling for all luminances. The lowest segment luminance was equal to background luminance. (**b**) With invisible apertures, spatiotemporal integration of contour motions is more difficult, lowering performance for the diamond from ceiling. At the slower speed (1.07°/s), performance for all shapes improves, with a shallow slope as segment luminance decreases. At the higher speed (2.14°/s), performance increases with a steeper slope, especially for the cross and chevron. The drop in performance at the lowest luminance level (3.79 cd/m^2, white symbols) is caused by the segments being close to detection threshold (a decrement due to poor visibility rather than to an inability to integrate the component motions).

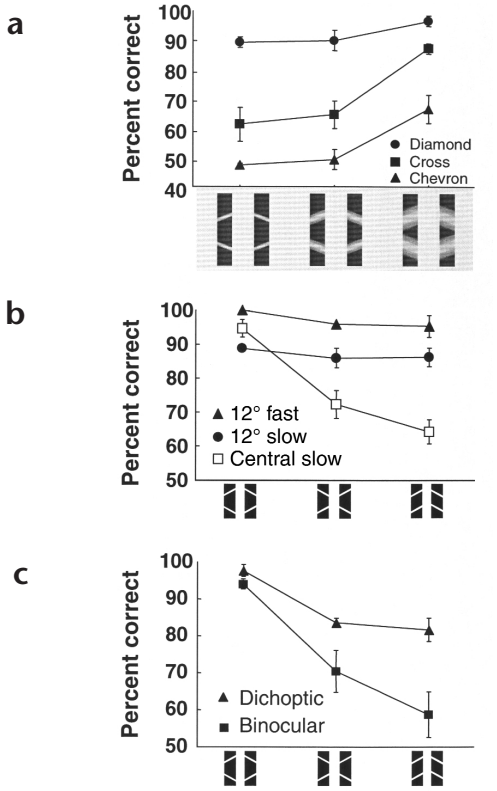

Fig. 5. Attenuated form–motion interactions. (**a**) Direction discrimination for diamond, cross and chevron shapes made of bars with Gaussian luminance profiles. The Gaussian's standard deviation was varied to produce nominal spatial frequencies of 8, 2 and 0.5 cpd (based on half-height frequency of Fourier spectra). Differences among shapes are large at high and medium spatial frequency and smaller at a low spatial frequency, mainly due to improved performance for the cross and chevron. (**b**) Direction discrimination in eccentric and central vision for the diamond, cross and chevron. At 12° eccentricity, differences among shapes are not significant. Performance is slightly better at the higher speed. Performance in central vision is presented for comparison and shows differences between shapes. (**c**) Direction discrimination for binocular and dichoptic presentation of the diamond, cross and chevron. In the dichoptic conditions, one of the diagonal pairs of contours (that is, upper-left/lower-right pair) was presented to one eye, and the other diagonal pair to the other eye. Previous dichoptic data (data not shown) indicate that the distribution of the contours between the eyes is not critical.

performance for the diamond as contour luminance decreased[13]. Performance for the cross and chevron again improved with decreasing luminance, and overall, there was a strong main effect of contour luminance ($F_{3,9} = 12.63$, $p < 0.002$). At the lowest luminance, contrast was about 3.5%, low enough to effectively bypass the parvo system[25]. Speed was also a significant factor; performance was better at the higher of the two speeds ($F_{1,3} = 14.0$, $p < 0.04$). Speed interacted with stimulus shape ($F_{2,6} = 6.61$, $p < 0.04$), with the slope of improving performance for the cross and chevron steeper at the higher speed.

Lowering spatial frequency also improves rotation discrimination ($F_{1,2} = 26.78$, $p < 0.005$). At high and medium frequencies (nominally 8 and 2 cycles per degree (cpd), based on the half-height frequency of their Gaussian-magnitude spectra), viewing the diamond elicited a level of performance different from viewing the cross or chevron. However, at low frequency (0.5 cpd), the shape-based distinction is attenuated, as performance improves markedly for difficult shapes. These data agree with a magno/parvo interpretation, as the two systems have similar sensitivities at moderate spatial frequencies (such as 2 and 8 cpd) yet diverge at lower frequencies, where sensitivity is much higher in the magno system[25]. In sum, the contrast and spatial frequency data imply that the parvo system prevents motion integration for difficult shapes. As conditions increasingly favor the magno system over the parvo system, performance for difficult shapes improves. As with the learning and priming data, this is consistent with an early form–motion interaction.

The question of early versus late interactions was explored further by comparing rotation discrimination in central and in near-peripheral (12° eccentric) vision. Varying eccentricity should not alter the relative contributions of form and motion pathways, as the relative mapping densities of the magno- and parvocellular systems do not vary with eccentricity[26]. However, as neurons in higher-level areas in both dorsal and ventral paths show position invariance[27,28], their responses should be similar regardless of stimulus location. A late form–motion interaction, then, would predict similar performance in central and eccentric vision. In contrast, the results (**Fig. 5b**) show that the large differences found in the preceding experiments between easy and difficult shapes are not observed at 12° eccentricity. Whereas speed was a significant main effect ($F_{1,3} = 150.9$, $p < 0.0012$), overall, differences between shapes were not ($F_{2,6} = 2.14$, n.s.), and performance averaged 92%. The null result for shape was not due to poor visibility, as the shapes were of high contrast and easily identifiable at this eccentricity. Moreover, high contrast had previously generated very strong form–motion interactions (compare **Figs. 2** and **3**). The effect of shape, then, depends on position in the visual field, inconsistent with a late influence of form on global motion. Finally, comparing performance for dichoptically versus binocularly viewed shapes reveals that dichoptic viewing markedly increases performance for difficult shapes (**Fig. 5c**). Dichoptic conditions effectively bypass the earliest levels of cortical processing because the complete shape is not available until binocular stages of processing. Because this condition attenuates the effect of shape on global motion integration, the influence of shape must (at least in part) arise in early cortical processing.

Discussion

Our results demonstrate that form has a critical and early role in global motion computation. Binding moving contours into global motion is an easy task for some shape configurations (diamonds) but difficult for others (crosses and chevrons; **Fig. 2**). Yet, more than just being difficult to integrate, our data suggest that there is something about the form of the 'difficult' shapes that actually impedes motion integration. This differs from previous studies that have shown that form–motion interactions generally occur reciprocally[6,7] at higher cortical levels[8]. In contrast, our data, based on a highly controlled set of motion stimuli, indicate a low-level, unidirectional influence of shape in determining whether motion integration is allowed to proceed or not.

Several arguments suggest that shape's influence on motion integration occurs early rather than late. To begin with, discriminating rotation of 'difficult' shapes cannot be learned or primed, implying that the limiting factor does not arise in higher stages in which cognitive strategies can be used. Also, the failure to obtain position invariance suggests extrastriate cortical areas are not involved. In contrast, the influence of shape on motion binding can be reduced by manipulating low-level stimulus properties

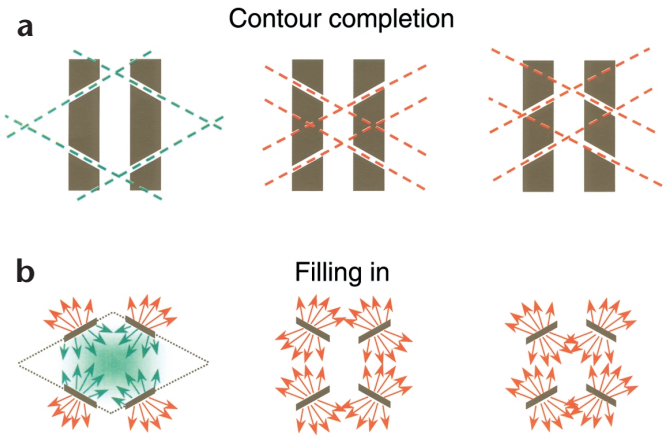

Fig. 6. Contour extrapolation (amodal completion), and surface filling-in for the diamond, cross and chevron. Both processes occur as early as primary visual cortex. (**a**) For diamond-like shapes (1, 4, 5 and 9 in **Fig. 1a**), contour extrapolation results in good closure (green lines) and thus permits surface filling-in (**b**, green arrows). This would result in a salient global object; consequently, judgments of global coherence for this shape were high. Also, as the diamond provides good closure, there would be no veto of motion integration, and hence, discrimination of rotation direction is very good. For open shapes (2, 3, 6, 7, 8 and 10 in **Fig. 1a**), contour extrapolation produces non-intersecting parallel and radial lines (red lines), which would not support closure and boundary-contingent filling-in. In the absence of closure, the filling-in process propagates without constraint, and eventually dissipates[37] (red arrows). This impoverished representation in the form domain generates weak coherence; it is associated with poor spatiotemporal integration in the motion domain.

(contrast, spatial and temporal frequency) to decrease the contribution of the parvocellular 'form' system, and by using dichoptic presentation to bypass the earliest cortical stages. Together, the data indicate an early form–motion interaction.

Evidence for a unidirectional influence of shape on motion comes from improved performance for 'difficult' shapes when stimuli favored the magno over the parvo system. Whether this is achieved by decreasing contrast and spatial frequency or by increasing temporal frequency, performance for difficult shapes improves toward the level seen with the diamond (**Figs. 4** and **5**). This indicates the following: first, that what was preventing motion integration of difficult shapes related to the parvocellular stream, and second, that in terms of motion integration, the so-called difficult shapes are not really 'difficult' at all. The second conclusion is not so surprising. As the stimuli are all composed of identical local motions, it is sensible that they converge toward the same performance level as the influence of form diminishes. The first conclusion, however, is less obvious and points to an importance for the parvocellular stream in global motion computation. Apparently, this role is to regulate whether motion integration is carried out or not, as attenuating the parvocellular system renders previously 'difficult' shapes 'easy,' as if motion integration is suddenly allowed to proceed.

The implication is that when form information is present, global motion integration is gated by a low-level and form-based process. Contours implying convex, closed forms (good Gestalts) are given the 'green light' for motion integration, whereas contours implying open, concave forms trigger a veto that prevents motion binding. We found no evidence for a corresponding facilitatory effect of shape. Conceivably, one reason why the diamond yields good performance might be that good form facilitates motion integration. However, our manipulations designed to weaken the form system's contribution improved performance for all shapes—the diamond as well as the 'difficult' shapes. Improved performance for the diamond would not be predicted if the diamond were benefiting from a form-based facilitation. If it were, weakening the form response (and hence its facilitatory effect) would have reduced performance. As performance improves for all shapes, we speculate that motion integration proceeds by default if there is no veto signal from the form system.

What purpose would be served by empowering form processes with the right of veto over motion integration? In short, it would help prevent integration of local motions not belonging together, which is especially a risk when they are spatially separated or partially occluded. Blind integration of local retinal motions would inevitably result in spurious combinations, creating an unstable and non-predictive perception with disastrous consequences for the organism. Using information from non-motion sources reduces this risk, guiding the motion system before it activates its powerful motion integration processes. In effect, if a probable form cannot be constructed, it is unlikely the local motion signals belong to the same 'object' and so motion integration should not proceed. Open, convex shapes are examples of improbable shapes; their contours cannot be joined without turning points and sharp curvatures (that is, they are not 'relatable'[29]). For this reason, creating shapes with four independent motion components instead of just two (**Fig. 3a**) did not help the motion system resolve global rotation if the contours implied open forms.

A motion integration veto would need to be made early. This would explain why 'difficult' shapes remained poorly performed despite extended practice and full-shape priming. The lack of perceptual learning was not anticipated because learning for specific shapes is observed in physiological studies of higher form areas such as IT[30], as well as in psychophysical studies[31]. However, if integration for 'difficult' shapes were vetoed early, then learning in higher-level form areas would be prevented. Consistent with this, closed diamond-like shapes were the only ones to show perceptual learning. Another unanticipated result was that priming failed to improve performance. We reasoned that knowing the exact form of the occluded shape would render the local motions more intelligible. Again, an early veto makes sense of this unexpected result, as influences from higher cognitive levels would not alter performance if motion integration were expressly vetoed at an early stage.

Apart from being good forms in the Gestalt sense, what is the significance of closed shapes to the visual system? A contour extrapolation process such as amodal completion would divide our stimuli into two shape classes that correspond to our performance-based distinction between 'easy' and 'difficult' shapes. For the diamond, contour extrapolation defines a closed, convex shape, whereas for the cross or chevron, open, concave shapes are produced (**Fig. 6**), in which contours radiate and never intersect. Cells in V1 respond to contours rendered discontinuous by occlusion[32] and so could subserve amodal completion of the diamond. Several factors might then account for superior performance for this stimulus. One is that processes of perceptual grouping are highly sensitive to closure[33,34]. Another is that once the diamond's boundary is amodally completed, the process of filling in (that is, the allocation of surface attributes to enclosed regions) would occur. This would endow the diamond with greater salience as a visual form than open shapes, and would square with our data showing the diamond is perceived most coherently.

Psychophysical experiments[35,36] and computational modeling[37,38] indicate that amodal completion between partially occluded contours (as in our stimuli) is sufficient to constrain filling-in processes. Filling-in is initiated by boundary completion and thus would not occur with open, concave shapes. Moreover, neural evidence shows the processes of contour completion and of boundary-initiated surface formation occur as early as V1 (ref. 39). Cooperative interactions between neighboring, relatable contours[16,29,40,41] and the long-range horizontal connections in V1 (refs. 42, 43) thought to underlie them are likely also to be involved in these processes, possibly by conducting a preshaping of elements into proto-forms. Thus, consistent with our low-level evidence, V1 neurons have the potential to extract relationships among contours, perform closure of the diamond and trigger its filling-in. More commonly, shape processing is discussed in terms of higher cortical areas such as V4 (refs. 44, 45) and IT[46]. Whereas these areas feed back into V1 and could help guide a low-level process[47], they are unlikely by themselves to provide the substrate indicated by our data.

Finally, we do not propose that form and motion interact only at low levels. As noted above, interactions at higher levels have been reported[8], and indeed, form and motion may interact at many levels within the visual system depending on stimulus and task requirements. In addition, global motion is possible without global form perception in stimuli such as random-dot kinematograms. These are essentially pure motion stimuli devoid of form, and as our data show, motion integration proceeds by default in the absence of form. Occluded shapes, however, being composed of line segments, contain the ingredients for a form–motion interaction. With these stimuli, we find that global motion integration is gated by a low-level, form-based process that vetoes motion integration when closed shapes cannot be established.

Methods

The stimuli, binocularly viewed on a Sony GDM1950 monitor ($1280 \times 1024 \times 8$ bits) at 60 Hz, were white (101 cd/m^2) outlined shapes presented within two black vertical apertures within a gray (2.73 cd/m^2) surrounding occluder hiding their vertices (**Fig. 1a**). All shapes were derived from a single diamond stimulus by permuting one or more component contours (for example, permuting the diamond's lower contours creates a chevron) or by adding a vertical offset. Two shapes were constructed by rotating the contours of shapes 5 and 6 by 20°. Except for the latter 2 shapes, contours were all identical (orientation, 30° and 150°; length, 1.27 degrees visual angle; width, 1/60 degrees visual angle). All shapes were rigid and underwent a global translation along a circular path. The spatial frequency spectra and total energy of the shapes were therefore essentially identical (**Fig. 1b**), with differences concerning only the phase spectra. The contour permutations did, however, affect apparent closure of the shapes, as well as altering higher-order characteristics such as the convexity of the global form and the relatability of neighboring contours (that is, the extent to which contour extrapolation produces vertices).

Four subjects, including the authors, served as observers. Their task (**Fig. 1c**) was to discriminate clockwise versus counterclockwise direction of a randomly chosen shape translating around a circular path at 1.07°/s (0.5 rev/s) when viewed from 114 cm. A path radius of 0.34 degrees visual angle ensured that the vertices of all shapes remained invisible. Duration was 0.5 s (1/4 cycle) with starting points randomized. Individually, the contours contained no rotational component. Thus, observers had to integrate contour motions over space and time to recover rotation direction. All shapes (except the rotated ones) had an identical velocity space representation (**Fig. 1d**). Finally, the number, velocity and (average) eccentricity and separation of the contour terminations were identical for all the shapes. Thus, models accounting for another aperture-viewed stimulus, the barber-pole effect, in terms of propagating contour terminators[48,49] would not be able to account for any differences among shapes in our experiments. All experimental procedures were within the ethical guidelines of the research institution.

In experiment 1, 4 observers discriminated rotation direction for 10 shapes (**Fig. 1a**; each block represents 400 trials; 2 directions × 10 shapes × 20 trials). Eight blocks of trials without feedback were performed on different days, followed by five blocks with negative feedback. The following experiments were structured similarly to experiment 1, but modified slightly. In experiment 2, 4 shapes (**Fig. 3a**) each made of 4 segments at different orientations (30°, 150°, 110° and 70°) were used. Shapes 1 and 5 (and 2 and 4) were constructed by exchanging the location of the lower segments. A triangle shape was also included. In experiment 3, only 3 shapes (diamond, cross and chevron) were used. On each trial, the full, unoccluded and stationary shape was presented for one second before the vertices were hidden and rotation began. Experiment 4a used only the diamond, cross and chevron at 4 segment luminance levels (2.73, 12.6, 31.1, 58.9 cd/m^2). Aperture luminance was zero, and background luminance was 2.73 cd/m^2. Experiment 4b was like experiment 4a, except that aperture and background had equal luminance, rendering apertures invisible. Segment luminances were 3.79, 4.87, 8.83 and 18.97 cd/m^2. Two speeds (1.07°/s and 2.14°/s) were tested. Experiment 5 differed from experiment 1 in that the shapes (diamond, cross and chevron) were made of bars with Gaussian luminance profiles of different widths. In experiment 6, the stimuli (diamond, cross and chevron) were randomly presented 12° left or right of central fixation. Two speeds (1.07°/s and 2.14°/s) were tested. In experiment 7, the stimuli (diamond, cross and chevron) were viewed dichoptically or binocularly. In dichoptic conditions, one of the diagonal pairs of contours (that is, upper-left/lower-right pair) was presented to one eye, and the other diagonal pair to the other eye.

Acknowledgements

Supported by the CNRS and by a Long-Term Fellowship from Human Frontiers Science Programme to D.A. Thanks to D. Shulz and Y. Frégnac for discussions.

RECEIVED 26 JANUARY; ACCEPTED 24 MAY 2001

1. Ungerleider, L. G. & Mishkin, M. in *The Analysis of Visual Behavior* (eds. Ingle, D. J., Mansfield, R. J. W. & Goodale M. S.) 549–586 (MIT Press, Cambridge, Massachusetts, 1982).
2. Livingstone, M. S. & Hubel, D. H. Psychophysical evidence for separate channels for the perception of form, color, movement and depth. *J. Neurosci.* **11**, 3416–3468 (1987).
3. DeYoe, E. A. & Van Essen, D. C. Concurrent streams in monkey visual cortex. *Trends Neurosci.* **11**, 219–226 (1988).
4. Geesaman, B. J. & Andersen, R. A. The analysis of complex motion patterns by form/cue invariant MSTd neurons. *J. Neurosci.* **16**, 4716–4732 (1996).
5. Braddick, O. J., O'Brien, J. M. D., Wattam-Bell, J., Atkinson, A. & Turner, R. Form and motion coherence activate independent, but not dorsal/ventral segregated, networks in the human brain. *Curr. Biol.* **10**, 731–734 (2000).
6. Anderson, B. L. & Sinha, P. Reciprocal interactions between occlusion and motion computations. *Proc. Natl. Acad. Sci. USA* **94**, 3477–3480 (1997).
7. Watanabe, T. Velocity decomposition and surface decomposition: reciprocal interactions between motion and form processing. *Vision Res.* **37**, 2879–2889 (1997).
8. Tse, P., Cavanagh, P. & Nakayama, K. in *High-Level Motion Processing—Computational, Neurobiological and Psychophysical Perspectives* (ed. Watanabe, T.) 245–266 (MIT Press, Cambridge, Massachusetts, 1998).
9. Rao, S. C., Rainer, G. & Miller, E. K. Integration of what and where in the primate prefrontal cortex. *Science* **276**, 821–824 (1997).
10. Malpeli, J. G., Schiller, P. H. & Colby, C. L. Response properties of single cells in monkey striate cortex during reversible inactivation of individual lateral geniculate laminae. *J. Neurophysiol.* **46**, 1102–1119 (1981).
11. Nealy, T. A. & Maunsell, J. H. R. Magnocellular and parvocellular contributions to the responses of neurons in macaque striate cortex. *J. Neurosci.* **14**, 2069–2079 (1994).
12. Sawatari, A. & Callaway, E. M. Convergence of magno- and parvocellular pathways in layer 4B of macaque primary visual cortex. *Nature* **380**, 442–446 (1996).
13. Lorenceau, J. & Shiffrar, M. The influence of terminators on motion integration across space. *Vision Res.* **32**, 263–273 (1992).
14. Alais, D., van der Smagt, M. J., van den Berg, A. V. & van de Grind, W. A. Local and global factors affecting the coherent motion of gratings presented in multiple apertures. *Vision Res.* **38**, 1581–1591 (1998).
15. Shiffrar, M. & Lorenceau, J. Increased motion linking across edges with decreased luminance contrast, edge width and duration. *Vision Res.* **36**, 2061–2068 (1996).

16. Lorenceau, J. & Zago, L. Cooperative and competitive spatial interactions in motion integration. *Vis. Neurosci.* **16**, 755–770 (1999).
17. Morgan, M. J., Findlay J. M. & Watt, R. J. Aperture viewing: a review and a synthesis. *Q. J. Exp. Psychol.* **34A**, 211–233 (1982).
18. Adelson, E. H. & Movshon, J. A. Phenomenal coherence of moving visual patterns. *Nature* **300**, 523–525 (1982).
19. Wilson, H. R. & Kim, J. A model for motion coherence and transparency. *Vis. Neurosci.* **11**, 1205–1220 (1994).
20. Guilford, J. P. *Psychometric Methods* (New York, McGraw-Hill, 1954).
21. Merigan, W. H. & Maunsell, J. H. How parallel are the primate visual pathways? *Annu. Rev. Neurosci.* **16**, 369–402 (1993).
22. Shapley, R. Visual sensitivity and parallel retinocortical channels. *Annu. Rev. Psychol.* **41**, 635–658 (1990).
23. Tootell, R. B. *et al.* Functional analysis of V3A and related areas in human visual cortex. *J. Neurosci.* **17**, 7060–7078 (1997).
24. Shimojo, S., Silverman, G. & Nakayama, K. Occlusion and the solution to the aperture problem for motion. *Vision Res.* **29**, 619–626 (1989).
25. Derrington, A. M. & Lennie, P. Spatial and temporal contrast sensitivities of neurones in lateral geniculate nucleus of macaque. *J. Physiol. (Lond.)* **357**, 219–240 (1984).
26. Livingstone, M. S. & Hubel, D. H. Do the relative mapping densities of the magno- and parvocellular systems vary with eccentricity? *J. Neurosci.* **11**, 4334–4339 (1987).
27. Duffy, C. J. & Wurtz, R. H. Response of monkey MST neurons to optic flow stimuli with shifted centers of motion. *J. Neurosci.* **15**, 5192–5208 (1995).
28. Sereno, A. B. & Maunsell, J. H. R. Shape selectivity in primate lateral intraparietal cortex. *Nature* **395**, 500–503 (1998).
29. Kellman, P. J. & Shipley, T. F. A theory of visual interpolation in object perception. *Cognit. Psychol.* **23**, 141–221 (1991).
30. Miyashita, Y. & Hayashi, T. Neural representation of visual objects: encoding and top-down activation. *Curr. Opin. Neurobiol.* **10**, 187–194 (2000).
31. Sigman, M. & Gilbert, C. D. Learning to find a shape. *Nat. Neurosci.* **3**, 264–269 (2000).
32. Sugita, Y. Grouping of image fragments in primary visual cortex. *Nature* **401**, 269–272 (1999).
33. Kovacs, I. & Julesz, B. A closed curve is much more than an incomplete one: effect of closure in figure-ground segmentation. *Proc. Natl. Acad. Sci. USA* **90**, 7495–7497 (1993).
34. Elder, J. H. & Zucker, S. W. Evidence for boundary-specific grouping. *Vision Res.* **38**, 143–152 (1998).
35. Yin, C., Kellman, P. J. & Shipley, T. F. Surface completion complements boundary interpolation in the visual integration of partly occluded objects. *Perception* **26**, 1459–1479 (1997).
36. Rensink, R. A. & Enns, J. T. Early completion of occluded objects. *Vision Res.* **38**, 2489–2505 (1998).
37. Grossberg, S. & Mingolla, E. Neural dynamics of form perception: boundary completion. *Psychol. Rev.* **92**, 173–211 (1985).
38. Grossberg, S. Cortical dynamics of three-dimensional figure-ground perception of two-dimensional pictures. *Psychol. Rev.* **104**, 618–658 (1997).
39. Lamme, V. A., Rodriguez-Rodriguez, V. & Spekreijse, H. Separate processing dynamics for texture elements, boundaries and surfaces in primary visual cortex of the macaque monkey. *Cereb. Cortex* **9**, 406–413 (1999).
40. Field, D. J., Hayes, A. & Hess, R. F. Contour integration by the human visual system: evidence for a local "association field." *Vision Res.* **33**, 173–193 (1993).
41. Polat, U. & Sagi, D. The architecture of perceptual spatial interactions. *Vision Res.* **34**, 73–78 (1994).
42. Gilbert, C. D. Horizontal integration and cortical dynamics. *Neuron* **9**, 1–13 (1992).
43. Kapadia, M. K., Ito, M., Gilbert, C. D. & Westheimer, G. Improvement in visual sensitivity by changes in local context: parallel studies in human observers and in V1 of alert monkeys. *Neuron* **15**, 843–856 (1995).
44. Pasupathy, A. & Connor, C. E. Responses to contour features in Macaque area V4. *J. Neurophysiol.* **82**, 2490–2502 (1999).
45. Gallant, J. L., Connor, C. E., Rakshit, S., Lewis, J. W. & Van Essen, D. C. Neural responses to polar, hyperbolic, and Cartesian gratings in area V4 of the macaque monkey. *J. Neurophysiol.* **76**, 2718–2739 (1996).
46. Kobatake, E. & Tanaka, K. Neuronal selectivities to complex object features in the ventral visual pathway of the macaque cortex. *J. Neurophysiol.* **71**, 856–867 (1994).
47. Hupé, J. M. *et al.* Cortical feedback improves discrimination between figure and background by V1, V2 and V3 neurons. *Nature* **394**, 784–787 (1998).
48. Hildreth, E. & Koch, C. The analysis of visual motion: From computational theory to neuronal mechanisms. *Annu. Rev. Neurosci.* **10**, 477–533 (1987).
49. Yuille, A. L. & Grzywacz, N. M. A computational theory for the perception of coherent visual motion. *Nature* 333, 71–74 (1988).